Journal of Thermal Analysis and Calorimetry, Vol. 56 (1999) 437–446

EFFECT OF HEATING RATE ON CRYSTALLIZATION KINETICS OF AMORPHOUS $Al_{91}La_5Ni_4$ ALLOYS BY DSC

*L. Soifer and E. Korin**

Department of Chemical Engineering, Ben-Gurion University of the Negev, P.O. Box 653 Beer-Sheva, 84105, Israel

Abstract

Crystallization kinetics of $Al_{91}La_5Ni_4$ amorphous ribbons produced by a melt-spinning method were studied by DSC analysis and X-ray diffraction. The effect of heating rate (from 4 to 200°C min^{-1}) was investigated in the temperature range from 298 to 700 K. Increases the heating rate from 4 to 200°C min^{-1} resulted in increases of the temperature difference between the two stages of the transformation process: crystallization of Al and crystallization of the Al compounds from 148.9 to 167.4 K. The apparent activation energies for the first step, related to Al crystallization, and to the second step related to crystallization of Al_4La and Al_3Ni, were found to be 161±9 and 199±10 kJ mol^{-1}, respectively. The results indicate the possibility of tailoring the heating treatment to produce the required fraction of the amorphous phase.

Keywords: Al–La–Ni amorphous ribbons, DSC, heating rate, non-isothermal crystallization kinetics

Introduction

For the last several years Al-based amorphous alloys have been used as raw materials for produced high mechanical strength nanocrystalline alloys [1–5]. It was found that the crystallinity of the alloy has a significant effect on its properties. For example, optimum strength was obtained for partial amorphous alloys, which contains about 25% (volume fraction) crystalline aluminum in the alloy [6]. There are several method to produce the desirable crystalline to amorphous ratio in amorphous ribbons produced by melt-spinning method such as: a) controlling the cooling rate of the fused alloys at the melt-spinning stage [2–4], b) the thermal treatment of melted alloys before rapid quenching [7], c) annealing of the amorphous materials [8–9] and d) possible combinations of the method mentioned above. In all techniques the crystallization kinetics is required as basic data for design the process. The experimental studies shows that in most cases such as: $Al_{(90\text{-}80)}Fe_{(7\text{-}30)}Nb_{(3\text{-}10)}$ [10]; $Al_{86}Ni_{10}Zr_2$, $Al_{86}Fe_{10}Zr_4$ [11] – the Al-based amorphous alloys crystallized in two stages: the first stage crystallization – precipitation of the crystalline; the second stage crystallization –

* Author to whom all correspondence should be addressed.

1418–2874/99/ $ 5.00

Akadémiai Kiadó, Budapest
Kluwer Academic Publishers, Dordrecht

transformation of the remaining amorphous matrix to intermetallic crystalline compounds.

Among the many Al-based alloys, the ternary system Al La In has the best combined mechanical strength and corrosion resistance properties [12]. Inoue *et al.* [12] carried out crystallization kinetics studies of compositions defined by the formula $Al_{90-x}La_{10}Ni_x$. Manov *et al.* [13] studies the crystallization process of $Al_{91}La_5Ni_4$ amorphous alloy by DTA at heating rate 4°C min^{-1}. In our previous paper, the effect of the overheating conditions of the molten $Al_{91}La_5Ni_4$ alloy-exposure time and temperature before the rapid quenching step was investigated [7]. The heating rate is one of the most important design parameters in crystallization process. However, the effect of heating rate on crystallization of $Al_{91}La_5Ni_4$ was not studied.

The work focuses on investigation of the effect of heating rate on crystallization of amorphous $Al_{91}La_5Ni_4$ ribbons prepared by the rapid quenching method.

Experimental

The amorphous $Al_{91}La_5Ni_4$ ribbons with a cross-section 0.015×4.00 mm were prepared as described previously by Manov *et al.* [13]. The procedure consists of the following three stages: i) aluminum, lanthanum and nickel are melted in an Al_2O_3 crucible (mass 47–52 mg) under an Ar atmosphere; ii) the cooled alloy is remelted at a rate of 40°C min^{-1} in an arc furnace under a He atmosphere to facilitate homogeneous mixing; iii) soaked this melt for 10 min at 1473 K and followed by 5 min at 1373 K; and iiii) amorphous ribbons are produced by rapid quenching, which is achieved by forcing the melt on to a copper drum.

DSC analysis of 4–5 mg samples were performed by Mettler Toledo DSC 820 System. The instrument was calibrated with pure indium (melting temperature 429.9 K, heat fusion 28.4 J g^{-1}). The analysis were performed under a nitrogen atmosphere (99.9% pure) at heating rates 4, 8, 15, 25, 50, 100 and 200°C min^{-1} in a temperature range of 298 to 700 K. The structures of the phases were determined by X-ray diffraction with a PW 1050/70 Philips X-ray Diffractometer with CuK_α radiation at a constant temperature of 298±1 K.

The specimens from the ribbons at different stages of DSC analysis were examined. The specimens were quenched in an oil bath to reduce the effect of transit cooling time of the specimens.

Results and discussion

DSC analysis and X-ray diffraction were used to study the effect of heating rate on crystallization kinetics of amorphous ribbons of $Al_{91}La_5Ni_4$. Figure 1 shows the DSC curves for heating rate of 4, 8, 15, 25, 50, 100 and 200°C min^{-1}. Two exothermic peaks were observed in all curves. The X-ray diffraction patterns for amorphous $Al_{91}La_5Ni_4$ ribbon as obtained after the quenching step and in heating process after the first and the second peak of the DSC curve is shown in Fig. 2. The broad halos of the diffractogram obtained before DSC analysis indicate that the ribbon has X-ray

amorphous structure. The diffraction pattern of the sample related to heating up to 540 K (after the first peak) shows that Al is the only crystalline phase, whereas the diffraction pattern of the sample related to heating up to 670 K (after the second peak) shows that Al, Al_4La and Al_3Ni crystalline phases exist. This result is consistent with other experimental work on Al based amorphous alloys that the crystallization process has been divided into two steps: crystallization of Al phase followed by crystallization of intermetallic compounds.

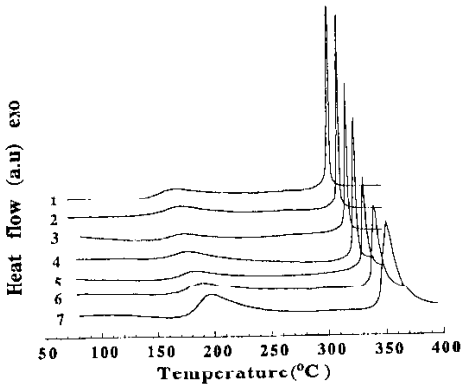

Fig. 1 DSC curves of $Al_{91}La_5Ni_4$ ribbons for different heating rate: 1 – 4°C min^{-1}, 2 – 8°C min^{-1}, 3 – 15°C min^{-1}, 4 – 25°C min^{-1}, 5 – 50°C min^{-1}, 6 – 100°C min^{-1}, 7 – 200°C min^{-1}

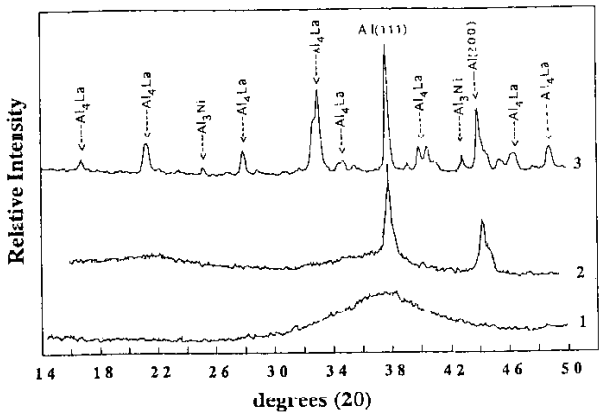

Fig. 2 X-ray diffractograms for $Al_{91}La_5Ni_4$ alloys. Curve 1 – before DSC analysis, curve 2 – after heating to 520 K and curve 3 – after heating to 670 K at a heating rate of 50°C min^{-1}

Table 1 summarizes the effect of heating rate on the following parameters: temperature of start of the first stage of crystallization (T_x), temperature of start of the second stage of crystallization (T_{cr}), temperature of the maximum of the first DSC peak (T_{p1}), temperature of maximum of the second DSC peak (T_{p2}), the temperature difference between ($\Delta T_p = T_{p2} - T_{p1}$), heat of crystallization for the first stage (ΔH_{p1}), heat of crystallization of the second stage (ΔH_{p2}). Figure 3 shows ΔT_p *vs.* the heating rate. The increase of heating rate from 4 to 50°C min^{-1} resulted increase the value of the ΔT_p from 148.9 to 161.7 K thereafter the effect is insignificant reached to only 167.4 at 200°C min^{-1}. By extrapolation of these plots to zero heating rate by logarithm equations, the values of ΔT_p at infinitesimal heating rate were determined to be 142.4 K.

Table 1 Effect of heating rate (β) on characteristic parameters of DSC curves for $Al_{91}La_5Ni_4$ amorphous ribbons

β/ °C min^{-1}	T_x/	T_{cr}/	T_{p1}/	T_{p2}/	ΔT_p/	ΔH_{p1}/	ΔH_{p2}/
			K			kJ mol^{-1}	
4	393.0	559.1	425.5	574.4	148.9	1.45	2.74
8	395.8	570.7	432.6	583.9	151.3	1.80	2.70
15	402.6	579.2	439.0	592.8	153.8	2.39	2.67
25	412.1	589.2	440.3	599.4	159.1	2.16	2.59
50	417.5	597.8	446.6	608.3	161.7	1.98	2.49
100	429.9	606.6	457.1	618.4	161.3	1.67	2.44
200	442.7	615.3	463.8	632.2	167.4	1.49	2.42

T_x temperature of the first stage of crystallization, T_{cr} temperature of the second stage of crystallization, T_{p1} temperature of the maximum of the first DSC peak, T_{p2} temperature of the maximum of the second DSC peak, ΔT_p the temperature difference between T_{p2} and T_{p1}, ΔH_{p1} heat of first stage of the crystallization, ΔH_{p2} heat of second stage of the crystallization

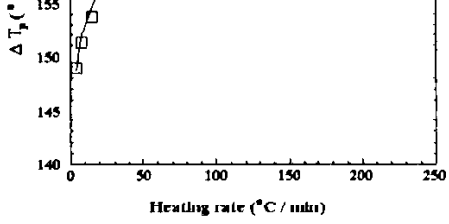

Fig. 3 Temperature difference between T_{p2} and T_{p1} *vs.* heating rate

In this case, the increase in heating rate from 4 to 200°C min^{-1} resulted the non-monotonous change in the heats of crystallization of Al : increases from 1.45 to 2.39 kJ mol^{-1} in the heating rate range of 4 to 15°C min^{-1} and decreases monotonically to 1.49 kJ mol^{-1} in the heating rate range of 15 to 200°C min^{-1}. This values of heat crystallization of Al are in the same order of magnitude as reported by others, Al crystallization from other amorphous alloys such as [14]: 0.84 kJ mol^{-1} for alloy $Al_{87}Ni_7Fe_7Ce_3$; 1.3 kJ mol^{-1} for alloy $Al_{87}Ni_{10}Ce_3$ and 1.8 kJ mol^{-1} for alloy $Al_{87}Ni_8Ag_2Ce_3$. The heat of crystallization of Al compounds decreased from 2.67 to 2.42 kJ mol^{-1} as in the heating rate range increase from 4 to 200°C min^{-1}.

The apparent activation energies for the crystallization processes were estimated by the Kissinger 'peak shift' method. The activation energies calculated from the slopes of the fitted linear function of $\ln(\beta/T_p^2)$ *vs.* $1/T_p$ for crystallization of Al and crystallization of aluminum compounds were 161±9 and 199±10 kJ mol^{-1}, respectively (Fig. 4).This value for the activation energies of crystallization of the Al is within the range of (138–174 kJ mol^{-1}) which reported in [15] for amorphous $Al_{87}Ni_{10-x}(Cu,Ag)Ce_3$. It is important to note that value of the activation energy of crystallization of the Al is close to that for lattice diffusion Q_L in aluminum 142 kJ mol^{-1} [16]; this might indicate that the crystallization rate dominated by diffusion process.

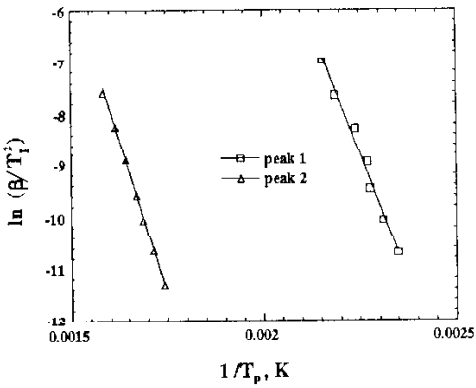

Fig. 4 Kissinger plot $\ln(\beta/T_p^2)$ *vs.* $1/T_p$ for first and second DSC peaks

The procedure suggested in [17] for analysis crystallization kinetics of non isothermal heating process is adopted for the analysis of the experimental data of crystallization of Al and Al-compounds.

The functions $y(\alpha)$ and $z(\alpha)$ was determined by Eqs (1) and (2).

$$y(\alpha) \cong (d\alpha/dt) \exp(E_\alpha/RT) \quad (1)$$

$$z(\alpha) \cong (d\alpha/dt)T^2 \quad (2)$$

The local activation energy E_α, was calculated from Eq. (3), [18].

$$\ln(d\alpha/dt)_\alpha = \ln A_1 - (E_\alpha/RT) \quad (3)$$

where α fraction crystallized, t is the time, T is the temperature (K), R is the gas constant, A_1 is pre-exponential coefficient.

The values of the pre-exponential coefficient ($\ln A_1$), reduced activation energy (E_α/R), activation energy (E_α) and Pearson linear correlation coefficients (r^2) are summarized in Table 2. The values of local activation energy for Al crystallization are practically constant in the interval between $0.1<\alpha<0.8$ and the mean value is

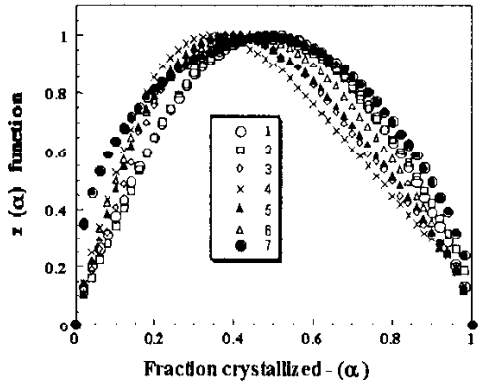

Fig. 5 The normalized $z(\alpha)$ function for Al phase crystallization at different heating rate: 1 – 4°C min^{-1}, 2 – 8°C min^{-1}, 3 – 15°C min^{-1}, 4 – 25°C min^{-1}, 5 – 50°C min^{-1}, 6 – 100°C min^{-1}, 7 – 200°C min^{-1}

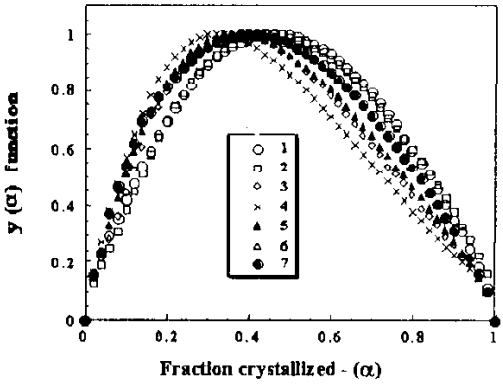

Fig. 6 The normalized $z(\alpha)$ function for Al phase crystallization at different heating rate: 1 – 4°C min^{-1}, 2 – 8°C min^{-1}, 3 – 15°C min^{-1}, 4 – 25°C min^{-1}, 5 – 50°C min^{-1}, 6 – 100°C min^{-1}, 7 – 200°C min^{-1}

E_α=157.3±8.3 kJ mol^{-1}. The values of local activation energy for Al-compounds phase crystallization are practically constant in the interval 0.05<α<0.7, and the mean value of local activation energy is E_α=187.3±6.2 kJ mol^{-1}. These values are in good agreement with the values calculated by Kissinger method: 161±9 and 199± 10 kJ mol^{-1}, respectively.

Normalized function of $y(\alpha)$ and $z(\alpha)$, at different heating rates, for crystallization of Al are given in Figs 5 and 6, and for Al-compounds crystallization in Figs 7 and 8. It is clear, that for Al and Al-compounds crystallization, the shape of both $y(\alpha)$ and $z(\alpha)$ functions is convex for all heating rates. The maximum of the $z(\alpha)$ function α_p^∞ and

Table 2 The pre-exponential coefficient (ln$A$), reduced activation energy (E_α/R), activation energy (E_α) and the Pearson linear correlation coefficient (r^2), calculated by isoconversional method for Al and Al-compounds crystallization

α	ln(A/s^{-1})	E_α/R (K)10^3	r^2	E_α/ kJ mol^{-1}
		Al crystallization		
0.05	40.306	15.570	0.969	129.4
0.10	44.006	17.380	0.980	144.5
0.20	46.499	18.755	0.981	155.9
0.30	47.611	19.472	0.977	161.9
0.40	48.164	19.928	0.966	165.7
0.50	48.004	20.077	0.946	166.9
0.60	46.086	19.466	0.885	161.8
0.70	44.470	18.989	0.857	157.6
0.80	40.003	17.293	0.760	143.8
0.90	32.144	13.928	0.607	115.8
0.95	27.459	11.916	0.526	99.1
		Al-compounds crystallization		
0.05	30.298	23.599	0.940	196.2
0.10	29.622	23.343	0.980	194.1
0.20	28.858	22.586	0.864	187.8
0.30	28.411	22.681	0.994	188.6
0.40	28.109	22.562	0.966	187.6
0.50	27.895	22.510	0.995	187.2
0.60	26.900	21.874	0.992	181.8
0.70	25.501	21.067	0.988	175.2
0.80	23.713	20.022	0.982	166.3
0.90	20.707	18.275	0.972	151.9
0.95	18.777	17.179	0.958	142.8

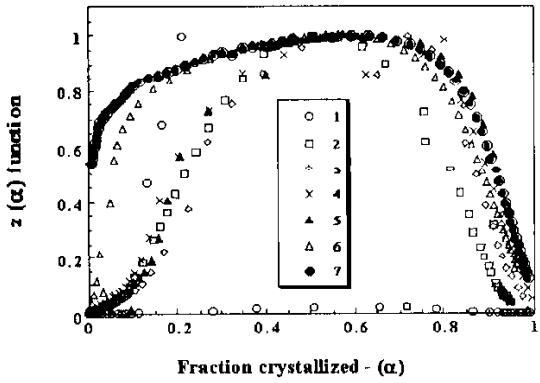

Fig. 7 The normalized $z(\alpha)$ function for Al-compounds phase crystallization at different heating rate: 1 – 4°C min^{-1}, 2 – 8°C min^{-1}, 3 – 15°C min^{-1}, 4 – 25°C min^{-1}, 5 – 50°C min^{-1}, 6 – 100°C min^{-1}, 7 – 200°C min^{-1}

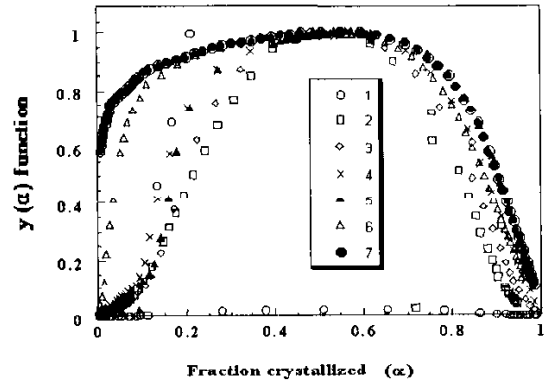

Fig. 8 The normalized $y(\alpha)$ function for Al-compounds phase crystallization at different heating rate: 1 – 4°C min^{-1}, 2 – 8°C min^{-1}, 3 – 15°C min^{-1}, 4 – 25°C min^{-1}, 5 – 50°C min^{-1}, 6 – 100°C min^{-1}, 7 – 200°C min^{-1}

$y(\alpha)$ function α_M for both crystallization process are summarized in Table 3. It shows that the location of the maximum depends on heating rates. For Al crystallization the values of α_p^∞ and α_M are in the interval between $0.34<\alpha_p^\infty<0.50$ and $0.30<\alpha_M<0.42$, respectively. For Al-compounds crystallization the values of α_p^∞ and α_M are in the interval between $0.21<\alpha_p^\infty<0.63$ and $0.21<\alpha_M<0.63$, respectively. According to reference [17], the most probable kinetic model is described by the Šesták-Berggren function [19]:

$$(d\alpha/dt)^* = \alpha^m(1-\alpha)^n \tag{4}$$

where $(d\alpha/dt)^*$ is normalized crystallization rate, m and n is empirical exponent, and p is kinetic parameter ratio defined by $p=m/n$.

The parameter p can be calculated by Eq. (5)

$$p = \alpha_M/(1 - \alpha_M) \tag{5}$$

The values of kinetic parameter ratio p for the two crystallization processes at different heating rates are given in the Table 3.

Table 3 The isoconversial kinetic parameters for Al and Al-compounds crystallization: the maxima of the $z(\alpha)$ function (α_p^∞) and $y(\alpha)$ function (α_M), the empirical kinetic parameter ratio ($p=m/n$) for Šesták-Berggren kinetic equation

β/ °C min^{-1}	Al crystallization			Al-compounds crystallization		
	α_p^∞	α_M	p	α_p^∞	α_M	p
4	0.50	0.46	0.85	0.21	0.21	0.27
8	0.48	0.48	0.92	0.51	0.51	1.04
15	0.38	0.38	0.61	0.49	0.49	0.96
25	0.34	0.30	0.43	0.63	0.63	1.70
50	0.38	0.34	0.52	0.56	0.56	1.27
100	0.42	0.42	0.72	0.51	0.49	0.96
200	0.48	0.42	0.72	0.54	0.51	1.04

It can be seen that in our case, the values of p depends on heating rate. Thus indicates that Šesták-Berggren function is not suitable to describe the non isothermal kinetic crystallization processes of amorphous $Al_{91}La_5Ni_4$ alloy. It is worthwhile to mention that pre-nucleators which effect the crystallization kinetic process (size less than 5 nm) might exist in the sample which could not be detected by X-ray diffraction. In addition, the analysis consider that the temperature in the samples is uniform, an assumption which is commonly used in DSC measurement. However, it is expected that the temperature gradient in the sample increases with increasing heating rates and might become significant at heating rates above 100°C min^{-1}. In order to adjust an appropriate kinetic model, additional experimental data are required, particularly in isothermal conditions.

Conclusions

The experimental results show that the heating rate has a significant influence on the crystallization kinetics of amorphous $Al_{91}La_5Ni_4$ ribbons obtained by rapid quenching. The specific conclusions that might be drawn from this study are:

1. Increasing the heating rate from 4 to 200°C min^{-1} results in an increase of the temperature difference between the two stages of the transformation process: crys-

tallization of Al and crystallization of the Al compounds from 148.9 to 167.4 K. This indicates the possibility of tailoring the heating treatment to produce the required fraction of the amorphous phase.

2. The apparent activation energies for the first step, related to Al crystallization, and to the second step, related to crystallization of Al_4La and Al_3Ni, were found to be 161±9 and 199±10 kJ mol^{-1}, respectively.

3. The heating rate parameter (4 to 200°C min^{-1}) has a significant effect on the crystallization kinetics of amorphous $Al_{91}La_5Ni_4$ alloy.

References

1 H. Chen, Y. He, G. J. Shiflet and S. J. Poon, Scripta Metallurg. Mater., 25 (1991) 1421.
2 Y. H. Kim, A. Inoue and T. Masumoto, Mater. Trans. JIM, 8 (1990) 747.
3 Y. H. Kim, A. Inoue and T. Masumoto, Mater. Trans. JIM, 32 (1991) 599.
4 Y. H. Kim, A. Inoue and T. Masumoto, Mater. Trans. JIM, 32 (1991) 331.
5 K. Higashi, T. T. Mukai, A. Uoya et al., Mater. Trans. JIM, 36 (1995) 1467.
6 A. L. Greer, Science, 267 (1995) 1947.
7 E. Korin, L. Soifer and V. Manov, J. Therm. Anal. Cal., 51 (1998) 361.
8 K. Higashi, T. T. Mukai, S. Tanimura et al., Scripta Metallurg. Mater., 26 (1992) 191.
9 K. Ohtera, A. Inoue, T. Terabayashi et al., Mater. Trans. JIM., 33 (1992) 775.
10 F. Audebert, H. Sirkin and A. G. Escorial, Scripta Mater., 36 (1997) 405.
11 M. Blank-Bewerrsdorf, J. Mater. Sci. Lett., 10 (1991) 1225.
12 A. Inoue, K. Ohtera and A-P. Tsai, Jpn. J. Appl. Phys., 27 (1988) L280.
13 V. Manov, A. Rubinshtein, A. Voronel, P. Popel and A. Vereschagin, Mat. Sci. Eng., A179/A180 (1994) 91.
14 A. Inoue, K. Nakazato, Y. Kawamura, A. P. Tsai and T. Masumoto, Mater. Trans. JIM, 33 (1994) 95.
15 A. P. Tsai, A. Inoue, Y. Bizen and T. Masumoto, Acta Metall., 37 (1989) 1443.
16 K. Hihashi, T.G. Niet, M. Mahuchi and J. Wadsworth, Scripta Metall. Mater., 32 (1995) 107.
17 J. Málek, Thermochim. Acta, 200 (1971) 257.
18 H. L. Fridman, J. Polym. Sci., C6 (1964) 183.
19 J. Šesták and G. Berggren, Thermochim. Acta, 3 (1971) 1.